Human LIM Domain Kinase 1 (LIMK1), Kinase Domain

A Target Enabling Package (TEP)

USEFUL LINKS

GeneCards HUMAN GENE DATABASE   Open Targets   50 YEARS OMIM Human Genetics Knowledge for the World   IMPC International Mouse Phenotyping Consortium   ChEMBL

(Please note that the inclusion of links to external sites should not be taken as an endorsement of that site by the SGC in any way)

SUMMARY OF PROJECT

Loss of the translational repressor FMRP in fragile X syndrome causes upregulation of the type II BMP receptor BMPR2 and its non-canonical signalling via the kinase LIMK1. LIMK1 performs inhibitory phosphorylation on cofilin proteins blocking their actin-severing activity. Excessive BMPR2-LIMK1 activation was associated with dendritic spine and behavioural defects in animal models that could be rescued by BMPR2 knockdown or LIMK1 inhibition. Here we present a target enabling package for the therapeutic target LIMK1. We include crystal structures of BMPR2, LIMK1, LIMK2 and the LIMK1-cofilin complex, as well as multiple assays for small molecule inhibitor screening. Finally, we identify a series of allosteric LIMK1 inhibitors with promising potency and selectivity that may potentially allow the development of a safe drug for this chronic indication.
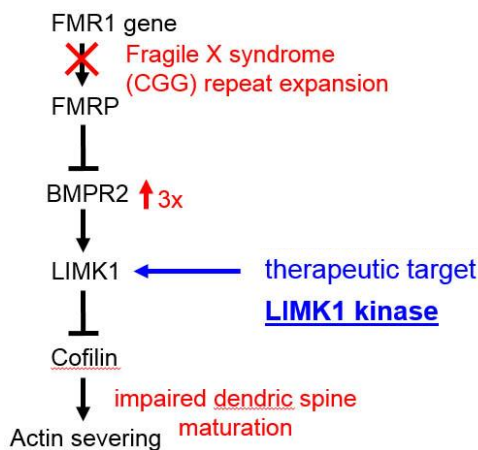
SCIENTIFIC BACKGROUND

Fig. 1. Schematic of LIMK1 upregulation

Fragile X syndrome is the most common heritable intellectual disability affecting 1 in 4000 males and 1 in 6000 females. (CGG)n repeat expansion in the *fragile X mental retardation 1* gene abrogates expression of the gene product FMRP. Loss of this RNA-binding translational repressor protein causes a significant upregulation of mRNA for a subset of genes regulating neuronal plasticity. A new report indicates that the bone morphogenetic protein (BMP) type II receptor BMPR2 is one of these genes and that the resulting downstream overactivation of the kinase LIMK1 is an actionable therapeutic target to alleviate many of the symptoms of fragile X syndrome (Fig. 1).

LIMK1 contains two N-terminal LIM domains and a PDZ domain that enable its recruitment to the BMPR2 C-terminal tail region where the LIMK1 kinase domain functions to perform inhibitory phosphorylation on cofilin proteins preventing their actin-severing activity (Fig. 2). Excessive levels of BMPR2 lead to overactivation of the BMPR2-LIMK1-Cofilin phosphorylation cascade leading to stabilised actin and abnormal synapse and dendritic spine development. BMPR2 knockdown or LIMK1 inhibition could rescue both the dendritic spine development and behavioural defects suggesting the LIMK1 kinase as a therapeutic target (1). Moreover, C9ORF72 gene expansions in ALS (amyotrophic Lateral Sclerosis) patients are similarly linked via Arf6/Rac1 to LIMK1/2 activation and cofilin phosphorylation (Fig. 2). Thus, LIMK1 is also supported as a promising therapeutic target in ALS (2).

LIMK1 recruitment to BMPR2
(Int. J. Mol. Sci. 2011, 12(12), 8924-8946)

LIMK1/2 domains

LIMK1 inhibition rescues dendritic spine formation
(Sci Signal 2016; 7, 431:ra58)

Excess p-Cofilin in ALS
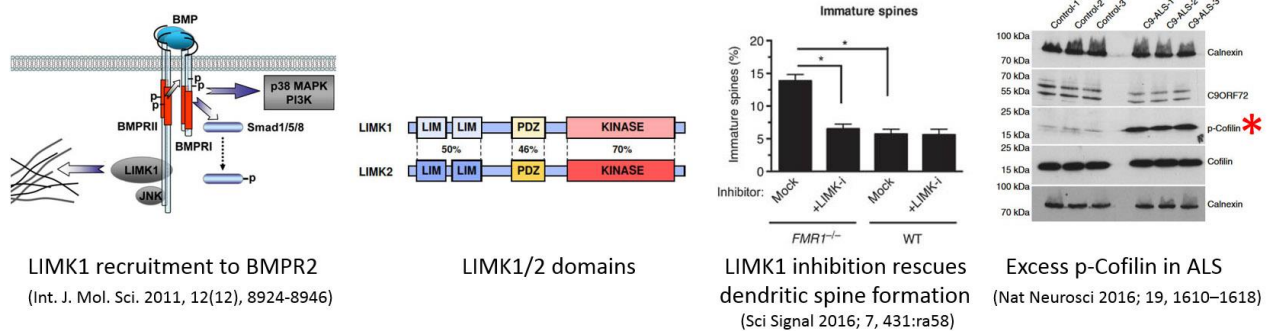(Nat Neurosci 2016; 19, 1610–1618)

Fig.2 Domains and (dys)function of LIMK1

To date kinase inhibitors have been directed towards LIMK2 and are poorly characterised against LIMK1 and against kinome-wide selectivity panels, or are otherwise likely too promiscuous for use in such a chronic indication. We aimed to (i) prepare relevant recombinant proteins; (ii) better characterise the BMPR2-LIMK1-cofilin pathway through structural and functional assays; (iii) identify potent and selective LIMK1 inhibitors that might form useful starting points for development of new treatments for Fragile X syndrome.

RESULTS – THE TEP

Proteins purified

CFL1 cofilin protein wild type (used for assays)
Full length human CFL1 was cloned into pNIC28-Bsa4, expressed in *E. coli* strain BL21(DE3)R3-pRARE2 and purified using Ni-affinity and size exclusion chromatography.

CFL1 cofilin protein Ser3Cys mutant (used for crystallography)
The Ser3Cys mutant was prepared similarly to the wild-type CFL1.

LIMK1 LIM-LIM domains (used for assays)
Human LIMK1 LIM-LIM domains (a.a. 18-172) were cloned into the vector pNIC-Zb, expressed in *E. coli* strain BL21(DE3)R3-pRARE2 and purified using Ni-affinity, size-exclusion and anion exchange chromatography.
BMPR2 kinase domain (used for crystallography)
Human BMPR2 (a.a. 189-517) was cloned into pNIC-CH, expressed in *E. coli* strain BL21(DE3)R3-pRARE2 and purified using Ni-affinity, size-exclusion and anion exchange chromatography.
LIMK1 kinase domain (used for crystallography and assays)
Human LIMK1 (a.a. 330-637) was cloned into pFB-LIC-Bse and prepared by baculoviral expression. LIMK1 protein was purified sequentially using Ni-affinity and size-exclusion chromatography. Further clean-up was performed by cation exchange chromatography or by reverse Ni-affinity chromatography following removal of the N-terminal hexahistidine tag.
LIMK2 kinase domain (used for crystallography and assays)
Human LIMK2 (a.a. 330-632) was cloned into pFB-LIC-Bse and prepared by baculoviral expression. LIMK2 protein was purified sequentially using Ni-affinity and size-exclusion chromatography.

Structural data

1. BMPR2 kinase + ADP/Mg^{2+} (3G2F, 2.35 Å)
2. LIMK1 kinase + ATPγS + Cofilin CFL1 (5L6W, 2.5 Å)
3. LIMK1 kinase + staurosporine (3S95, 1.65 Å)
4. LIMK1 kinase + PF-477736 (5NXC, 2.25 Å)
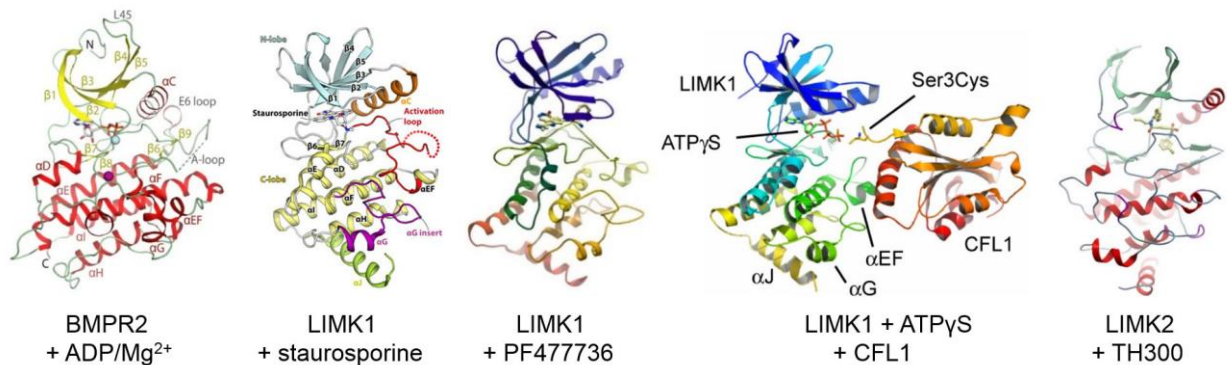5. LIMK2 kinase + TH300 (5NXD, 1.9 Å)

Fig. 3. Overview of structural data for this TEP

The LIMK family kinase fold exhibits a highly unusual structure with an atypical C-lobe adapted to bind to the cofilin substrate. Most interestingly, there is a loop insertion preceding the αG helix that effectively displaces the αG from the kinase substrate pocket allowing access for the globular cofilin (Fig. 4). An unusually positioned αJ helix is also present packing below the C-lobe. The functional significance of this remains to be determined, but hints at a further site for interaction. The LIMK1/2 kinase structures in complex with different inhibitors show that a variety of conformations can be targeted (Fig. 4):
(i) LIMK1-staurosporine shows a classic type I binding mode as expected with a DFG-in, αC-in conformation; (ii) LIMK1-PF477736 shows a DFG-in, αC-out conformation; (iii) LIMK2-TH300 shows an allosteric inhibitor binding mode to a DFG-out, αC-out kinase conformation. The structure of the BMPR2 kinase domain shows a constitutively-active conformation. Inhibitors targeting this domain may not be relevant for fragile X syndrome as LIMK1 binds to the large C-terminal tail of BMPR2 far from the kinase region. Attempts to crystallise the complex of LIMK1 with the BMPR2 tail were unsuccessful. The BMPR2 kinase domain structure is included for completeness.
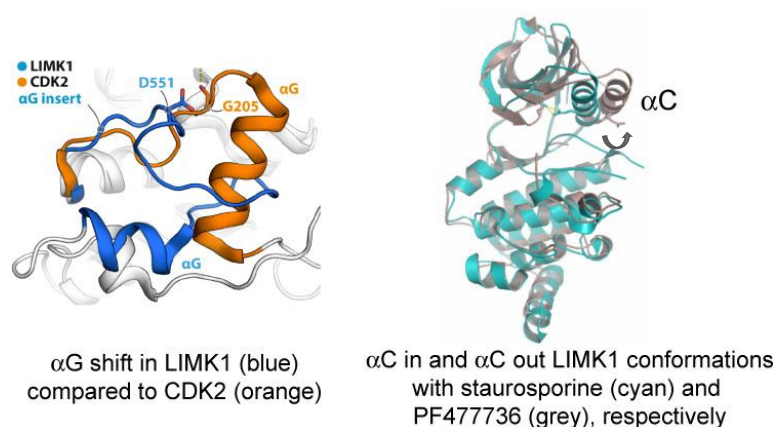
αG shift in LIMK1 (blue)
compared to CDK2 (orange)

αC in and αC out LIMK1 conformations
with staurosporine (cyan) and
PF477736 (grey), respectively

Fig. 4. Structural features of LIMK1

In vitro assays

1. ITC (isothermal titration calorimetry) mapping LIMK1 interaction site on the BMPR2 C-terminal tail
2. Thermal shift assay as an initial inhibitor binding screen
3. RapidFire Mass Spectrometry assay for inhibitor IC_{50} determination
4. ITC measurements of inhibitor binding
5. Collaborative drosophila models for fragile X syndrome

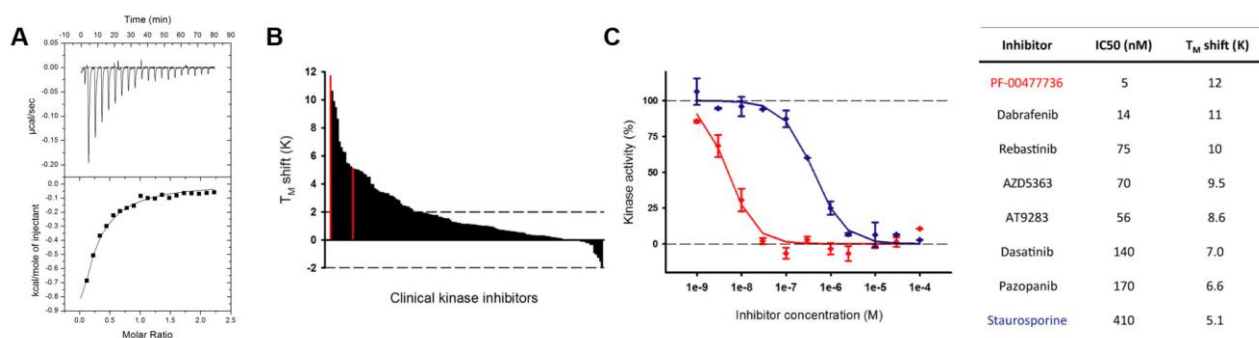| Inhibitor	IC50 (nM)	T_M shift (K)
PF-00477736	5	12
Dabrafenib	14	11
Rebastinib	75	10
AZD5363	70	9.5
AT9283	56	8.6
Dasatinib	140	7.0
Pazopanib	170	6.6
Staurosporine	410	5.1

Fig. 5. *In vitro* assays. (A) ITC measurement of the binding of the LIMK1 LIM-LIM domains (a.a. 18-172) to a BMPR2 peptide (SNLKQVETGVAKMNTINAA) shows a K_D value of 60 μM. (B) Summary plot of a thermal shift assay screen of ~150 clinical kinase inhibitors. Red lines indicate the range of inhibitors chosen for IC_{50} determination. (C) RapidFire mass spectrometry assay showing IC_{50} values for selected compounds.

LIMK1 interaction with the BMPR2 C-terminal tail
ITC experiments showed that the LIMK1 LIM-LIM domains (a.a. 18-172) can bind to the BMPR2 C-terminal region (a.a. 779-797) with a K_D value of 60 μM (Fig. 5).

***In vitro* kinase and inhibitor binding assays**
A fluorescence-based thermal shift assay (differential scanning fluorimetry) was performed as an initial screen to identify potential LIMK1 inhibitors. Selected hits ($T_m > 5°C$) were assessed further in *in vitro* kinase assays. These included a number of clinically-tested compounds (Fig. 5) as well as a number of putative allosteric inhibitors. Inhibitor IC_{50} values were determined using a RapidFire Mass Spectrometry-based assay established for LIMK1 and LIMK2 and their substrate cofilin (CFL1). The binding of the preferred chemical inhibitor TH251 was further characterised by ITC.

Collaborative drosophila models for fragile X syndrome
Our collaborator Akiko Hata has developed a drosophila larval crawling assay that can be used as a genetic or chemical screening platform for therapeutic molecules for fragile X syndrome. Larvae with loss-of-expression mutation of *dFMR1* had a significant increase in synaptic bouton formation in the larval neuromuscular junction as well as hyperactive crawling. A "LarvaTrack" algorithm was developed to automate analyses of locomotion videos to quantitate changes upon LIMK1 inhibition. Details are published in Sci Signal. 2017; 10, 477: eaai8133 (3).

Chemical starting points

Chemical matter with LIMK1 or LIMK2 co-crystal structures included type I inhibitors ATPγS and staurosporine, the clinically-tested compound PF-477736 and the allosteric inhibitor TH300.

TH251	ΔTm LIMK1 = 6.0°C	ITC LIMK1 = 53 nM
	IC_{50} LIMK1 = 52 nM	Ligand efficiency = 0.36
	IC_{50} LIMK2 = 47 nM	Ligand-lipophilicity efficiency = 3.11
TH255	ΔTm LIMK1 = 4.5°C	
TH300	ΔTm LIMK1 = 2.7°C	Ligand efficiency = 0.31
	IC_{50} LIMK1 = 413 nM	Ligand-lipophilicity efficiency = 1.73
	IC_{50} LIMK2 = 64 nM	
TH263	Inactive control	
	LIMK1 IC_{50} > 50 μM	
	LIMK2 IC_{50} > 50 μM	

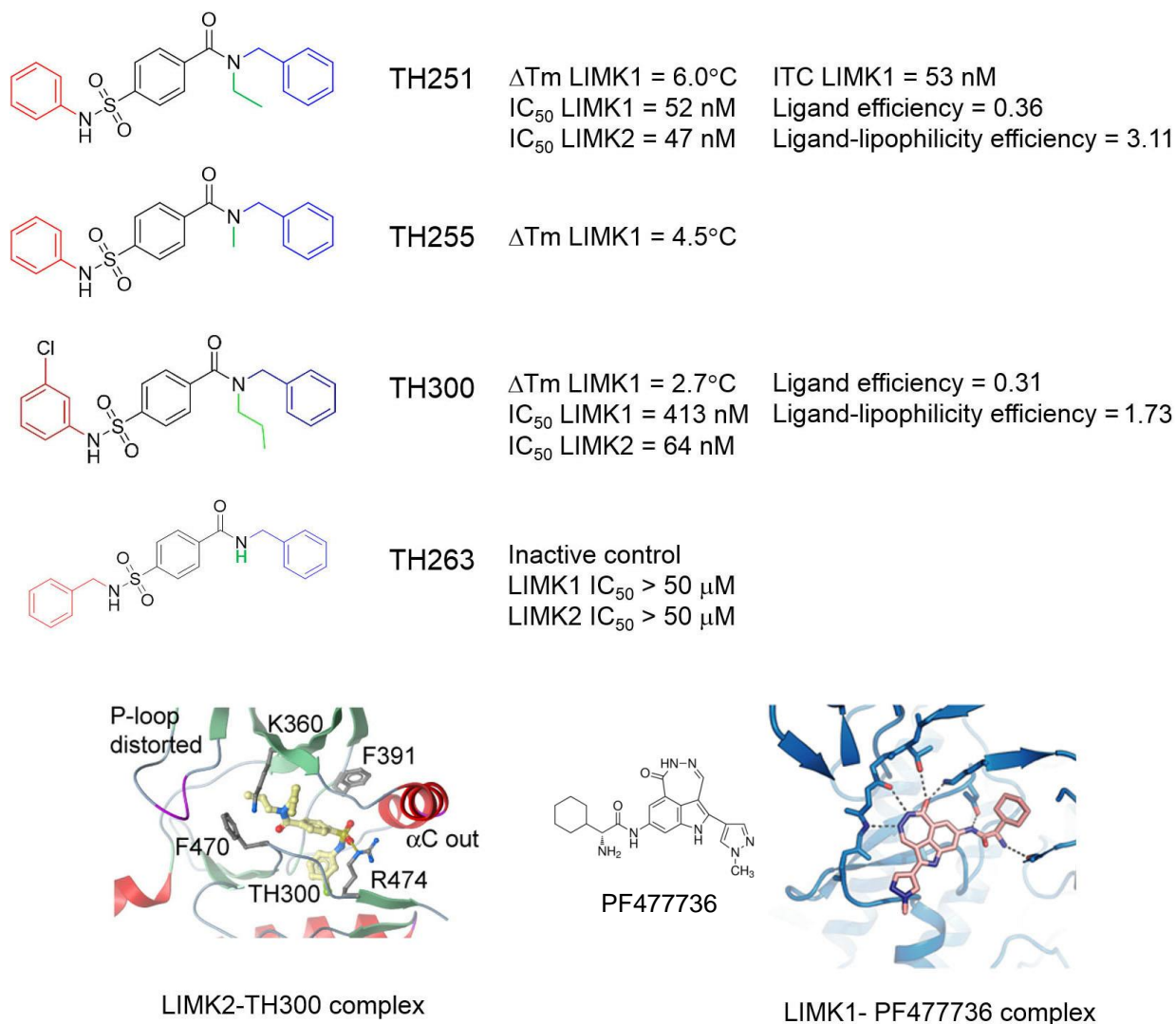LIMK2-TH300 complex

PF477736

LIMK1- PF477736 complex

Fig. 6. Chemical inhibitors of LIMK1

Our data suggest the chemical series containing TH251 as promising candidates for development. This series of allosteric LIMK1 inhibitors includes compounds that are both potent and selective, such as TH251 (Fig. 6).

IMPORTANT: Please note that the existence of small molecules within this TEP indicates that chemical matter can bind to the protein in a functionally relevant pocket. As such these molecules should not be used as tools for functional studies of the protein unless otherwise stated as they are not sufficiently potent or well-characterised to be used in cellular studies. The small molecule ligands are intended to be used as the basis for future chemistry optimisation to increase potency and selectivity and yield a chemical probe or lead series.

Antibodies

The following commercially-available antibodies may be helpful for work on LIMK1: LIMK1 (#3842, Cell Signaling); p-LIMK1/2 (#3841, Cell Signaling); Cofilin1 (#3318, Cell Signaling); p-Cofilin1/2 (#3311, Cell Signaling).

CRISPR/Cas9 Reagents

Reagents targeting human LIMK1 have been published by others in Nat Biotech (2016) 34, 184–191 and are available from Addgene (plasmids #76046, #76047, #76048, #76049).

New LIMK1/2 chemical probe

A new derivative of our TH-251 compound has been approved as a chemical probe for LIMK1/2. The datapack for this probe is available here:
https://www.thesgc.org/chemical-probes/TH-257
In a live cell NanoBRET assay (Promega) TH-257 has an IC_{50} of 250 nM against ectopically expressed full-length LIMK1 and 150 nM against LIMK2, respectively.

Future questions

• Further optimisation of TH251 chemical matter
• Further exploration of LIMK1 as a therapeutic target in fragile X syndrome and ALS models.

Collaborations:

• Chemistry partner: Stefan Knapp, Goethe-Universität, Frankfurt
• Drosophila assays: Akiko Hata, UCSF
• BMPR2-LIMK1 signalling: Petra Knaus, Freie Universität Berlin

CONCLUSION

Our work shows that LIMK1 has evolved distinct structural elements to allow recruitment to the BMPR2 C-terminal tail and interaction of the substrate cofilin protein. Our 2.5 Å structure of the LIMK1-CFL1 complex was enabled by inclusion of the non-hydrolysable ATPγS and by a Ser3Cys mutation in the CFL1 substrate site. Concurrently, a lower resolution (3.5 Å) structure of a LIMK1-CFL1 complex was solved and published by the group of Titus Boggon at Yale in Mol Cell 2016; 62, 397-408. Comparison of the two structures suggest a slight repositioning of the CFL1 as it engages the terminal phosphates.

Upregulation of the BMPR2-LIMK1-cofilin pathway in fragile X syndrome appears to drive synaptic and behavioural defects in animal models that phenocopy the human condition. Importantly, these could be rescued by the chemical inhibitors presented here (Fig. 7).
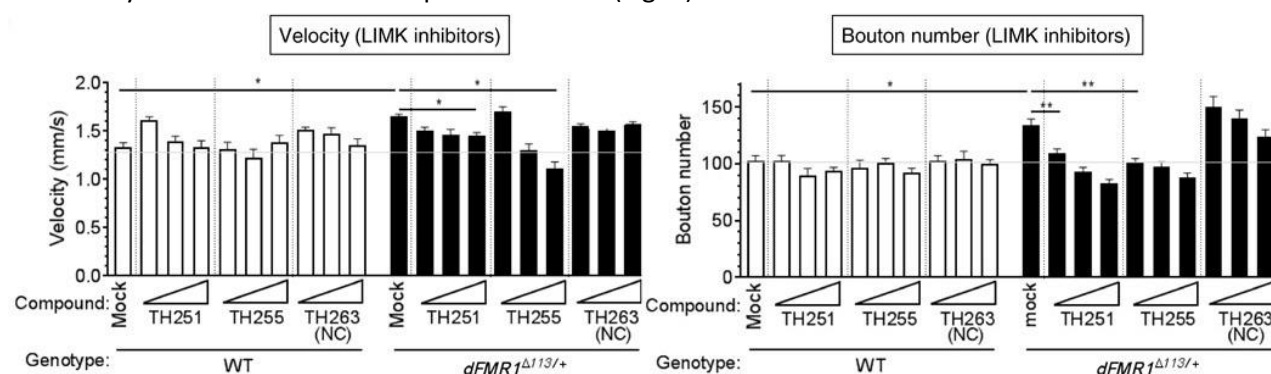

Fig. 7. LIMK1 inhibitors rescue the bouton and the crawling phenotypes in *dFMR1* mutants. Velocity and the neuromuscular junction bouton number were recorded in WT or mutant third-instar drosophila larvae treated with a active LIMK1 inhibitors (TH251 or TH255; 1, 5, or 50 µM) or an inactive analog (TH263). Further details can be found in the publication Sci Signal. (2017); 10(477). pii: eaai8133.

The allosteric inhibitor class was first reported by Lexicon (PDB 4TPT, (4)). Their compound was reported as selective for LIMK2 (IC_{50} = 39 nM) relative to LIMK1 (IC_{50} = 3.2 µM). Here, we show that the compound TH251 has significant potency for LIMK1 (IC_{50} = 52 nM) as well as excellent overall kinome-wide selectivity. Further

chemistry may be explored to assess opportunity for LIMK1-selectivity over LIMK2. It is noteworthy that relevant LIMK1 residues F411 and N455 are substituted to LIMK2 L403 and C446, respectively. The TH series compounds bind to an unusual inactive αC-out and DFG-out conformation where the DFG Phe inserts between P-loop and β3. This allosteric binding mode also allows opportunity to extend the compound towards the kinase hinge region. Further chemistry may also optimise the PK properties to facilitate future experiments in rodent models.

We also identified potent clinical inhibitors targeting LIMK1, including FDA-approved drug Dabrafenib (IC_{50} = 14 nM). This suggests that LIMK1 inhibition is viable in humans. However, these oncology drugs are still likely to be unsuitable for use in chronic diseases due to their promiscuous binding. The high selectivity of the allosteric inhibitor TH251 offers potentially improved future safety for use in Fragile X syndrome and perhaps ALS where similar LIMK-cofilin upregulation is reported (2).

Finally, other genes are also dysregulated in Fragile X syndrome and an mGlu5 inhibitor has also been shown to alleviate certain disease symptoms (5). Thus, in future selective LIMK1 and mGlu5 inhibitors could be tested in combination to test for additive protective effects.

Structure Files

PDB ID	Structure Details
3G2F	BMPR2 + ADP/Mg^{2+}
3S95	LIMK1 + staurosporine
5NXC	LIMK1 + PF-477736
5L6W	LIMK1 + ATPγS + Cofilin
5NXD	LIMK2 + TH300

Materials and Methods

Preparation of the Human LIMK1 LIM-LIM domains
Boundaries: residues 18-172
Vector: pNIC-Zb
Tag and additions: TEV-cleavable N-terminal hexahistidine and Z-basic tags
Expression cell: *E. coli* BL21(DE3)R3-pRARE2
Expression was performed in LB media containing 50 µg/mL kanamycin and 34 µg/mL chloramphenicol. Cultures were grown at 37°C with shaking until OD600 = 0.5 and then induced overnight at 18°C with 0.5 mM IPTG. Cells harvested and lysed by ultrasonication. Recombinant LIMK1 protein was purified on
Nickel-sepharose buffered in 50 mM HEPES pH 7.5, 500 mM NaCl, 5% glycerol, 0.5 mM tris(2-carboxyethyl)phosphine (TCEP) and eluted with an imidazole step gradient. Further purification was achieved using size-exclusion and anion exchange chromatography. Affinity tags were cleaved from LIMK1 using TEV protease.

Preparation of Human BMPR2 kinase domain
Boundaries: residues 189-517
Vector: pNIC-CH
Tag and additions: non-cleavable C-terminal hexahistidine tag
Expression cell: *E. coli* BL21(DE3)R3-pRARE2
The kinase domain of human BMPR2 (residues 189-517) was subcloned into the pNIC-CH vector and transformed into *E. coli* strain BL21(DE3)R3-pRARE2 for expression. This vector provides a non-cleavable
C-terminal hexahistidine tag. Cultures in LB media, 50 µg/mL kanamycin and 34 µg/mL chloramphenicol, were induced with 1 mM IPTG overnight at 18°C and the cells harvested and lysed by ultrasonication. Recombinant proteins were purified by Ni-affinity, size-exclusion and anion exchange chromatography. Proteins were stored at 4°C buffered in 50 mM HEPES pH 7.4, 300 mM NaCl, 10% glycerol, 10 mM DTT, 50 mM L-arginine, 50 mM L-glutamate.

Preparation of the Human LIMK1 kinase domain
Boundaries: residues 330-637
Vector: pFB-LIC-Bse
Tag and additions: TEV-cleavable N-terminal hexahistidine tag
Expression cell: Sf9 insect cells
Bacmid DNA was prepared from DH10Bac cells and used to transfect Sf9 insect cells for the preparation of initial baculovirus. LIMK1 protein was expressed from infected Sf9 cells cultivated in InsectXpress medium (Lonza) for 72 hours at 27°C. Harvested cells were resuspended in lysis buffer (50 mM HEPES pH 7.4, 500 mM NaCl, 20 mM imidazole, 0.5 mM TCEP, 5% glycerol) and lysed by sonication. The lysate was cleared by centrifugation and purified by Ni-affinity chromatography. LIMK1 was eluted in buffer supplemented to 300 mM imidazole. The eluted protein was cleaved overnight by TEV protease and purified further by size exclusion chromatography using an S200 16/600 column buffered in 20 mM HEPES pH 7.4, 500 mM NaCl, 5% glycerol, 0.5 mM TCEP. Additional clean-up was performed by reverse Ni-affinity chromatography and if necessary a cation exchange chromatography step using a HiTrap SP column. The final yield was 2 mg LIMK1 protein from 1L culture. It was observed that the inclusion of protease inhibitors during purification was helpful to maintain the intact LIMK1 protein.

Preparation of the Human LIMK1-CFL1 complex

For co-crystallisation the purified LIMK1 and CFL1 (Ser3Cys) proteins were mixed at a 1:1 molar ratio and incubated for 2 hours on ice. The complex was then purified by size exclusion chromatography using an AKTAxpress system with an S200 16/600 column buffered in 20 mM HEPES pH 7.4, 500 mM NaCl, 5% glycerol, 0.5 mM TCEP.

Preparation of the Human LIMK2 kinase domain

Boundaries: residues 330-632
Vector: pFB-LIC-Bse
Tag and additions: TEV-cleavable N-terminal hexahistidine tag
Expression cell: Sf9

Bacmid DNA was prepared from DH10Bac cells and using to transfect Sf9 insect cells for the preparation of initial baculovirus. LIMK2 protein was expressed from infected Sf9 cells cultivated in InsectXpress medium (Lonza) for 72 hours at 27°C. Harvested cells were resuspended in lysis buffer (50 mM HEPES pH 7.4, 500 mM NaCl, 20 mM imidazole, 0.5 mM TCEP, 5% glycerol) and lysed by sonication. The lysate was clarified by centrifugation and purified by Ni-affinity chromatography. LIMK2 was eluted in buffer supplemented to 300 mM imidazole. The eluted protein was cleaved overnight by TEV protease whilst being dialysed to remove imidazole. The cleaved protein was purified further using a reverse Ni-affinity purification step and then by size exclusion chromatography using an S200 16/600 column buffered in 20 mM HEPES pH 7.4, 500 mM NaCl, 5% glycerol, 0.5 mM TCEP. The final yield was 0.4 mg LIMK2 protein from 1L culture.

Preparation of full length Human CFL1 cofilin protein (wild-type and Ser3Cys mutant)

Boundaries: Full-length
Vector: pNIC28-Bsa4
Tag and additions: TEV-cleavable N-terminal hexahistidine tag
Expression cell: *E. coli* BL21(DE3)R3-pRARE2

A similar construct containing a Ser3Cys mutation was produced by site directed mutagenesis. Plasmids were transformed into *E. coli* strain BL21(DE3)R3-pRARE2. Expression was performed in LB media containing 50 µg/mL kanamycin and 34 µg/mL chloramphenicol. Cultures were grown at 37°C with shaking until OD600=0.5 and then induced overnight at 18°C with 0.5 mM IPTG. Cells were spun at 5000 rpm for 10 mins and the pellets frozen at -80°C. On thawing, cells were lysed by sonication and purified on Ni-sepharose resin in binding buffer (50 mM HEPES pH 7.4, 500 mM NaCl, 20 mM Imidazole, 5% glycerol, 0.5 mM TCEP). After washing with buffer supplemented to 50 mM imidazole, the CFL1 protein was eluted with buffer supplemented to 300 mM imidazole. The N-terminal affinity tag was removed by TEV cleavage overnight and the CFL1 protein purified further by size exclusion chromatography using an S200 16/600 column buffered in 20 mM HEPES pH 7.4, 500 mM NaCl, 5% glycerol, 0.5 mM TCEP. Fractions containing protein were pooled, concentrated and stored at -80°C.

Structure Determination of the BMPR2 kinase domain (PDB: 3G2F)

Crystallization of the BMPR2-ADP complex was achieved at 4°C using the sitting-drop vapour diffusion method. BMPR2 was pre-incubated with 10 mM ADP at a protein concentration of 5.8 mg/mL, and crystallized using a precipitant containing 25% PEG 8K, 0.3 M ammonium sulphate, 0.05 M $MgCl_2$, and 0.1 M sodium cacodylate pH 6.0. The diffraction quality co-crystals grew in a 150 nL crystallization drop containing equal volume of the protein and reservoir solution. Crystals were cryoprotected with mother liquor plus 20% ethylene glycol for the BMPR2-ADP complex and vitrified in liquid nitrogen. Diffraction data were collected at Swiss Light Source, station PX10 using monochromatic radiation at wavelength 1.000 Å. Data were processed with MOSFLM and subsequently scaled using the program SCALA from the CCP4 suite. Initial phases were obtained by molecular replacement using the program PHASER and the structure of ACVR2B (PDB 2QLU) as a search model. Density modification and NCS averaging were performed using the program DM, and the improved phases were used in automated model building with the programs ARP/wARP and Buccaneer. The resulting structure solution was refined using REFMAC5 from the CCP4 suite and manually rebuilt with COOT. Appropriate TLS restrained

refinement using the tls tensor files calculated from the program TLSMD was applied at the final round of refinement. The complete structure was verified for geometric correctness with MolProbity.

Structure Determination of the LIMK1 complex with staurosporine (PDB: 3S95)

Crystallization of LIMK1 was achieved by vapour diffusion using the sitting drop method at 20°C. The protein was pre-incubated with 1.5 mM staurosporine and concentrated to 8 mg/mL. Crystals were obtained mixing protein and reservoir at 3:1 volume ratio in 24% MPD, 100 mM Tris pH 7.2 and 10 mM phenol and were cryoprotected in 30% MPD, 10% glycerol. A diffraction dataset was collected at Diamond Light Source synchrotron, beamline I03, and indexed and integrated with MOSFLM. Scaling and merging were performed using the program SCALA. The structure was solved by molecular replacement using PHASER with the initial search models SRC (PDB 1YI6) and EPHA3 (PDB ID: 2QO9). Further manual model building used COOT, alternated with refinement using REFMAC5 in the CCP4 suite. Optimal TLS refinement was performed in the last refinement stages using parameters generated by the TLSMD server. The final model was validated with MOLPROBITY.

Structure Determination of the LIMK1 complex with PF-477736 (PDB: 5NXC)

10 mg/mL LIMK1 protein was mixed with 0.5 mM PF-477736. Crystals were grown at 4°C in sitting drops mixing 100 nL of the protein-ligand complex with 50 nL of a precipitant solution containing 0.1 M HEPES pH 7.0, 0.2 M MgCl$_2$, 10% PEG8K. Crystals appeared overnight and did not change appearance after 7 days. They were mounted in precipitant solution cryoprotected with 25% ethylene glycol. Data were collected at Diamond Light Source, analysed, scaled and merged with Xia2. The structure was solved by molecular replacement with PHASER using a SRC model as a template (PDB ID 1YI6) and refined with REFMAC. The model was validated using MOLPROBITY.

Structure Determination of the LIMK1-CFL1 complex with ATPγS (PDB: 5L6W)

10 mg/mL LIMK1-CFL1 protein complex was mixed with 1.2 mM ATPγS and 2.5 mg/mL MgCl$_2$. Crystals were grown at 4°C in sitting drops mixing 50 nL protein with 100 nL of a precipitant solution containing 0.1 M HEPES pH 7.5, 0.2 M KCl, 35% pentaerythritol propoxylate 5/4. Crystals were cryo-protected by equilibration into precipitant solution containing 20% ethylene glycol and vitrified in liquid nitrogen. Diffraction data were collected at Diamond, beamline I02, analysed, scaled and merged with Xia2. The structure was solved by molecular replacement with PHASER using a SRC model as a template (PDB ID: 1YI6) and refined with REFMAC5. The model was validated using MOLPROBITY.

Structure Determination of the LIMK2 complex with TH300 (PDB: 5NXD)

7.5 mg/mL LIMK2 protein was mixed with 0.5 mM TH300. Crystals were grown at 4°C in sitting drops mixing 75 nL of the protein-ligand complex with 75 nL of a precipitant solution containing 0.1 M BisTrisPropane pH 7.5, 0.2 M Na$_2$SO$_4$, 10% ethylene glycol, 17% PEG3.35K. Crystals appeared after 4 days and did not change appearance after 6 days. They were mounted in precipitant solution cryoprotected with an additional 20% ethylene glycol. Diffraction data were collected at Diamond Light Source, analysed, scaled and merged with Xia2. The structure was solved by molecular replacement with PHASER using a LIMK2 model as a template (PDB ID: 4TPT) and refined with REFMAC5. The model was validated using MOLPROBITY.

Thermal Shift Assay

A fluorescence-based thermal shift assay (differential scanning fluorimetry (DSF)) was performed as a screen to identify potential LIMK1 inhibitors. Ligands in this assay increase a protein's melting temperature (T_m shift) by an amount proportional to their binding affinity. A solution of 2 μM LIMK1 protein in assay buffer (20 mM HEPES pH 7.4, 150 mM NaCl, 0.5 mM TCEP, 5% glycerol) was mixed 1:1000 with SYPRO Orange (Sigma). Compounds to be tested were added to a final concentration of 10 μM. 20 μL of each sample were placed in a 96-well plate and heated from 25 to 95°C. Fluorescence was monitored using a Mx3005P real-time PCR instrument (Stratagene) with excitation and emission filters set to 465 and 590 nm, respectively. Data were analysed with the MxPro software and curves fit in Microsoft Excel using the Boltzmann equation to determine the midpoint of thermal denaturation (T_m). Thermal shift values (ΔT_m) induced by inhibitor binding were calculated relative to control wells containing protein and 2.5% DMSO.

RapidFire Mass Spectrometry Kinase Assay

An assay for inhibitor IC_{50} determination was developed using an Agilent 6530 Rapidfire QTOF Mass Spectrometer to follow LIMK1/2 kinase activity against the CFL1 substrate. RF-MS assays were performed in a 384-well plate format using polypropylene plates (Greiner, code 781280) and an assay buffer containing 50 mM TRIS pH 7.5, 0.1 mM EDTA, 0.1 mM EGTA. All bulk liquid handling steps were performed using a multidrop combi reagent dispenser (Thermo Scientific, Code 5840300) equipped with a small tube plastic tip dispensing cassette (Thermo Scientific, Code 24073290). After each reagent transfer, assay plates were sealed with an aluminium foil plate seal (Costar, Code 6570) and centrifuged briefly for 5 sec at 1000 rpm. For inhibitor IC_{50} determinations an 11-point and 3-fold serial dilution in DMSO was prepared from a 50 mM stock solution in DMSO and 250 nL of each concentration was transferred in duplicate using an ECHO 550 acoustic dispenser (Labcyte). A DMSO control (250 nL) was transferred into column 12 and the potent LIMK inhibitor, LIMKi3, was dispensed into column 24 as a no enzyme control. LIMK1 (80 nM, 2 X final concentration in assay buffer) and LIMK2 (400 nM, 2 X final concentration in assay buffer) was dispensed into each well of the assay plate (25 μl per well) and allowed to pre-incubate with inhibitor for 10 minutes at room temperature. After 10 minutes 25 μl of 2 X final concentration of substrate (1.6 mM ATP, 10 mM $MgCl_2$, 4 μM CFL1 in assay buffer) was dispensed into each well to initiate the reaction and the enzyme reaction was allowed to proceed for 1 hour (LIMK1) and 4 hour (LIMK2) at room temperature. The enzyme reaction was stopped by addition of 5 μl of 10% formic acid and the plate transferred to a RapidFire RF360 high throughput sampling robot. Samples were aspirated under vacuum and loaded onto a C4 solid phase extraction (SPE) cartridge and the SPE washed for 5.5 sec with 0.1% (v/v) formic acid in LCMS grade water to remove non-volatile buffer components. After the aqueous wash, analytes of interest were eluted from the C4 SPE onto an Agilent 6530 accurate mass Q-TOF in an organic elution step (85% acetonitrile in LCMS grade water containing 0.1% formic acid). Ion data for the CFL1 substrate and phosphorylated CFL1 product were extracted and peak area data integrated using RapidFire integrator software (Agilent). % conversion of CFL1 to phosphorylated CFL1 was calculated in excel and IC_{50} curves generated using graphpad prism version 7.0. The assay had a Z score of 0.69.

Isothermal Titration Calorimetry (ITC) using BMPR2 peptide

Experiments were performed at 15°C using a Microcal VP-ITC microcalorimeter. Proteins were buffered in 50 mM HEPES pH 7.5, 150 mM NaCl, 0.5 mM TCEP. 1 mM BMPR2 peptide (SNLKQVETGVAKMNTINAA) was titrated into a 100 µM solution of the LIMK1 LIM-LIM domains (a.a. 18-172). Data were analyzed using a single binding site model implemented in the Origin software package provided with the instrument.

Isothermal Titration Calorimetry (ITC) using TH251 inhibitor

Measurements were performed at 15°C on a MicroCal iTC200 (GE Healthcare). LIMK1 kinase domain was dialysed overnight into assay buffer (20 mM HEPES pH 7.4, 500 mM NaCl, 0.5 mM TCEP, 5% glycerol). The syringe was loaded with 150 µM LIMK1, the cell was filled with 15 µM TH-251. Every 2.5 minutes, 2 µL of the protein solution were injected into the cell for a total of 19 injections. The heat flow data were analysed with the MicroCal ORIGIN software package employing a single binding site model.

Intact mass spectrometry

Protein masses of all purified proteins were determined using an Agilent LC/MSD TOF system with reversed-phase high-performance liquid chromatography coupled to electrospray ionization and an orthogonal time-of-flight mass analyser. Proteins were desalted prior to mass spectrometry by rapid elution off a C3 column with a gradient of 5-95% isopropanol in water with 0.1% formic acid. Spectra were analysed using the MassHunter software (Agilent).

Drosophila models of Fragile X syndrome

A Drosophila model for fragile X syndrome was developed by the group of Akiko Hata. Hyperactive locomotion was demonstrated as a reliable behavioral marker for an *in vivo* drug screen. Full experimental details have been published (Sci Signal. 2017; 10, 477: eaai8133).

References

1. Kashima, R., Roy, S., Ascano, M., Martinez-Cerdeno, V., Ariza-Torres, J., Kim, S., Louie, J., Lu, Y., Leyton, P., Bloch, K. D., Kornberg, T. B., Hagerman, P. J., Hagerman, R., Lagna, G., and Hata, A. (2016) Augmented noncanonical BMP type II receptor signaling mediates the synaptic abnormality of fragile X syndrome. *Science signaling* **9**, ra58

2. Sivadasan, R., Hornburg, D., Drepper, C., Frank, N., Jablonka, S., Hansel, A., Lojewski, X., Sterneckert, J., Hermann, A., Shaw, P. J., Ince, P. G., Mann, M., Meissner, F., and Sendtner, M. (2016) C9ORF72 interaction with cofilin modulates actin dynamics in motor neurons. *Nature Neuroscience* **19**, 1610

3. Kashima, R., Redmond, P. L., Ghatpande, P., Roy, S., Kornberg, T. B., Hanke, T., Knapp, S., Lagna, G., and Hata, A. (2017) Hyperactive locomotion in a *Drosophila* model is a functional readout for the synaptic abnormalities underlying fragile X syndrome. *Science signaling* **10**

4. Goodwin, N. C., Cianchetta, G., Burgoon, H. A., Healy, J., Mabon, R., Strobel, E. D., Allen, J., Wang, S., Hamman, B. D., and Rawlins, D. B. (2015) Discovery of a Type III Inhibitor of LIM Kinase 2 That Binds in a DFG-Out Conformation. *ACS medicinal chemistry letters* **6**, 53-57

5. Hamill, S., Lou, H. J., Turk, B. E., and Boggon, T. J. (2016) Structural Basis for Noncanonical Substrate Recognition of Cofilin/ADF Proteins by LIM Kinases. *Molecular cell* **62**, 397-408